

Constant-Time Multidimensional Electrophoretic NMR¹

Ercheng Li² and Qihong He³

Department of Medical Physics, Memorial Sloan-Kettering Cancer Center, 1275 York Avenue, New York, New York 10021

Received July 3, 2001; revised April 17, 2002

Multidimensional electrophoretic NMR (ENMR) has been introduced to determine structures of coexisting proteins and protein conformations in solution. Signals of different proteins are separated in a new dimension of electrophoretic flow according to their characteristic electrophoretic mobilities. The electrophoretic interferograms have been generated in the flow dimension in two approaches by incrementing either the amplitude or the duration of the electric field. The ENMR method of incrementing the duration of the electric field, however, introduces severe signal decays due to molecular diffusion and spin relaxation, limiting the effectiveness of the method. In this study, an improved method of constant-time multidimensional ENMR (CT-ENMR) has been proposed and successfully tested. The time delays between the magnetic field gradients and the RF pulses are kept constant in this new method so that the molecular diffusion and spin relaxation processes contribute to only a constant factor of signal amplitude. As an alternative approach of incrementing the amplitude of the electric field, this novel method significantly enhances our capability and potential in characterizing structural changes of interacting proteins during biological signaling processes. The CT-ENMR method is particularly useful in studies where the amplitude-incrementing of the electric field is not optimal. For example, the CT-ENMR method is superior when the electric field is applied in the direction not parallel to the static magnetic field B_0 to the xy -magnetization. The new method was successfully demonstrated with a sample solution containing 100 mM 4,9-dioxo-1,12-dodecanediamine and 100 mM L-aspartic acid in D_2O . © 2002 Elsevier Science (USA)

Key Words: two-dimensional electrophoretic NMR; stimulated-echo; flow and convection; cylindrical ENMR sample cells; pulse field gradient NMR.

INTRODUCTION

Electrophoretic NMR (ENMR) (1–20) has a demonstrated potential in characterizing structures of coexisting proteins and protein conformations in solution (21–24). The overlapping

¹ Some of the preliminary results were reported in the 41th Experimental Nuclear Magnetic Resonance Conference (ENC), Asilomar, California, April 9–14, 2000.

² Current address: Department of Radiology, Howard University Cancer Center, Washington, DC, 20060.

³ To whom correspondence should be addressed at Memorial Sloan-Kettering Cancer Center, Department of Medical Physics, 1275 York Avenue, New York, NY 10021. Fax: (212) 717-3676. E-mail: heq@mkscc.org.

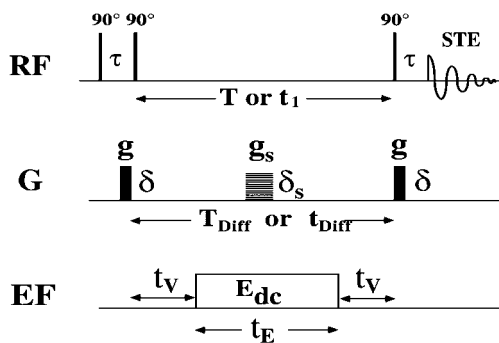
NMR signals of bovine serum albumin (BSA, 60 kD) and ubiquitin (8.6 kD) have been resolved without physical separation of the component proteins in solution (21). To investigate proteins in biological buffer conditions, capillary array ENMR (CA-ENMR) (22) and convection-compensated ENMR (CC-ENMR) have been developed (24) to remove spectral artifacts from heat-induced convection. The CA-ENMR sample tube also enhances the effective electric field, permitting ENMR measurements in solutions of high ionic strength. The multidimensional modality of ENMR, as demonstrated in a three-dimensional electrophoretic COSY (3D EP-COSY) experiment, provides structural information of molecules coexisting in the same solution (23). Such structural information is unavailable with the conventional multidimensional NMR methods. The signals from different molecules migrating in solution are modulated with the characteristic frequencies proportional to their electrophoretic mobilities. The NMR resonances from different molecules can be displayed at different *electrophoretic frequencies* in a new dimension of electrophoretic flow added to the traditional NMR spectrum that contains overlapping NMR resonances from all molecules in the mixture solution. Since the Hamiltonian governing spin dynamics commutes with that governing the electrophoretic flow motion of molecules, the separated NMR resonances from each molecular component are organized in the same way as in the corresponding NMR spectra from the pure single-component molecular solution. Therefore, the sorted NMR spectra can be analyzed in the conventional manner. In principle, structures of coexisting proteins can be obtained, even during their biochemical reactions.

The electrophoretic flow interferograms in the new dimension of nD-ENMR have been generated in two approaches: (a) using the electric field (EF)-time-incrementing method by increasing the duration of electric field pulse at a constant amplitude (1, 2), or (b) using the EF-amplitude-incrementing method by increasing the amplitude of the electric field at a fixed pulse duration (3, 21–24). However, the previous EF-time-incrementing method introduces severe signal decays from molecular diffusion and spin relaxation (1, 2), and most ENMR experiments prefer the EF-amplitude-incrementing approach since the time delays between the gradient and the RF pulses are constant and, therefore, the signal is free from the diffusion and relaxation decays (3, 8, 21). In this paper, we present an

improved EF-time-incrementing approach—the constant-time multidimensional ENMR (CT-ENMR) method—that removes the diffusion and relaxation signal decays. The time delays between the encoding and the decoding magnetic field gradients are fixed even though the duration of the electric field pulse increases. Therefore, the diffusion and relaxation processes contribute only constant amplitude factors to the electrophoretic interferograms, rather than exponential decays of the signal. The method was demonstrated with a sample solution containing 100 mM 4,9-dioxa-1,12-dodecanediamine and a 100 mM L-aspartic acid in D₂O. The novel method of CT-ENMR can be used when the EF-amplitude-incrementing ENMR is not appropriate or not optimal. For example, the CT-ENMR approach permits novel ENMR sample cell configurations that are not available in the EF-amplitude-incrementing methods. The CT-ENMR significantly enhances the technical capability and potential in characterizing the structures of coexisting proteins and protein interactions in solution.

THEORY

A modified two-dimensional (2D) stimulated-echo ENMR (STE-ENMR) pulse sequence (2) (Fig. 1) was designed to illustrate the concept of CT-ENMR. Similar modifications can be applied to other ENMR sequences to achieve the CT-ENMR ef-



Phase Cycling Procedure:

$\phi 1:$	$+x$	$+x$	$+x$	$+x$
$\phi 2:$	$-x$	$-x$	$-x$	$-x$
$\phi 3:$	$+x$	$+y$	$-x$	$-y$
ACQ:	$+x$	$+y$	$-x$	$-y$

FIG. 1. The 2D CT-STE-ENMR pulse sequence with constant time delays between the encoding and decoding gradients (T_{Diff}) and the RF pulses (T). The time period t_v flanking the electric field pulse is decreased in synchrony with the incrementing rate of the electric field pulse duration (t_E). The encoding and decoding gradients have the same amplitude (g) and duration (δ). The pulse sequence reduces to the previous EF-time-incrementing 2D STE-ENMR sequence when t_v is fixed and the time delays between the gradients (t_{Diff}) and RF pulses (t_1) change as the duration of the electric field pulse (t_E) increases.

fect. As in the original 2D STE-ENMR sequence (2), three 90° pulses are applied in the constant-time 2D STE-ENMR (CT-STE-ENMR) sequence. The first 90° pulse creates a transverse magnetization, which forms a helix after application of the first magnetic field gradient pulse of amplitude, g , with a duration, δ . This labels the spatial locations of spins and encodes the electrophoretic flow motion of ionic species. Half of the magnetization helix is stored in the z -direction by applying the second 90° pulse at time τ . During the z -storage time, the spin relaxation is dominated by the T_1 relaxation mechanism, which is relatively long compared to the T_2 relaxation time for proteins ($T_1 \gg T_2$) (6, 21, 22). The third 90° pulse flips the z -magnetization back to the xy -plane for signal detection. A decoding gradient is applied following the last 90° pulse to refocus the dephased magnetization and form a stimulated echo at time $2\tau + t_1$. The electrophoretic motion of a component molecule modulates the stimulated echo signal by a cosine factor, $\cos[(K E_{dc} t_E)\mu]$,

$$M(E_{dc}) = \frac{M(0)}{2} \exp\left[-DK^2\left(t_{Diff} - \frac{\delta}{3}\right) - \frac{2\tau}{T_2} - \frac{t_1}{T_1}\right] \times \cos[(K E_{dc} t_E)\mu], \quad [1]$$

assuming that a U-shaped ENMR sample chamber is used (2). The modulation cosinusoidal frequency is directly proportional to the electrophoretic mobility (μ), which is a characteristic property of the migrating molecule in solution. The parameter $K = \gamma g \delta$ characterizes the tightness of the magnetization helix. The amplitude of the DC electric field, $E_{dc} = I_e/(\kappa A)$, is determined by electric current (I_e), solution conductivity (κ), and the cross-sectional area (A) of the electrophoretic sample cell. The exponential term collects the contributions from the spin-spin relaxation process (T_2) during the τ interval, the spin-lattice relaxation effect (T_1) during the t_1 period, and molecular diffusion (D) between the dephasing and the refocusing gradients during the time delay, t_{Diff} . The spectral artifacts from the primary and secondary echoes are removed by a spoil gradient pulse of amplitude, g_s , with a duration, δ_s , in the z -storage period, where $g_s \delta_s > 4g\delta$ (2).

In the EF-amplitude-incrementing STE-ENMR, the electric field amplitude (E_{dc}) is stepwise increased to generate cosinusoidal modulations of signal amplitude in the flow dimension. The diffusion time (t_{Diff}) between the encoding and the decoding gradients remains constant and so do the time delays τ and t_1 between the RF pulses for spin relaxation in the transverse (T_2) and longitudinal (T_1) directions. Cosinusoidal amplitude modulations of each migrating species in solution are observed,

$$M(E_{dc}) = M_A \cos[(K E_{dc} t_E)\mu], \quad [2]$$

where the amplitude of the magnetization

$$M_A = \frac{M(0)}{2} \exp\left[-DK^2\left(t_{Diff} - \frac{\delta}{3}\right) - \frac{2\tau}{T_2} - \frac{t_1}{T_1}\right] = \text{Constant} \quad [3]$$

remains constant, which summarizes the contributions from molecular diffusion and spin relaxation processes to the electrophoretic interferograms. Resonances in the flow dimension are, therefore, free of diffusion and relaxation broadenings in the Fourier domain so that high spectral resolution can be obtained to differentiate signals from different molecules. This strategy has been effectively demonstrated when the overlapping signals from mixed proteins BSA and ubiquitin in solution were resolved by electrophoretic mobilities (21).

In the previous 2D EF-time-incrementing STE-ENMR (2), the pulse duration of electric field (t_E) is chosen as an incrementing variable. As t_E increases, the diffusion time delay (t_{Diff}) and T_1 relaxation period (t_1) increase proportionally. As a result, a severe exponential signal decay is superimposed to the electrophoretic oscillation curves. The exponential decays are translated to a line-broadening factor in the Fourier domain (I). In the new CT-ENMR method, the time delays (t_V) flanking the electric field pulse were stepwise decreased at the same rate synchronized with the incrementing rate of the electric field pulse duration (t_E). This process ensures a constant T_1 relaxation time delay, $T = t_E + 2t_V$, between the last two 90° pulses, as well as a constant diffusion time period, T_{Diff} , between the encoding and the decoding gradients in the ENMR experiments. The exponential term in Eq. [1] reduces to a constant factor, M_B , as t_E increases in CT-STE-ENMR:

$$M(E_{dc}) = M_B \cos[(K E_{dc} t_E) \mu], \quad [3]$$

where

$$M_B = \frac{M(0)}{2} \exp\left[-DK^2\left(T_{Diff} - \frac{\delta}{3}\right) - \frac{2\tau}{T_2} - \frac{T}{T_1}\right] \\ = \text{Constant} \quad [4]$$

is the amplitude of the magnetization weighted by a constant diffusion and relaxation factor, which has a value determined by the 2D CT-STE-ENMR experimental parameters. Similar to the EF-amplitude-incrementing 2D ENMR method, the CT-ENMR experiment produces electrophoretic oscillation curves of constant amplitudes. Both are free from diffusion and relaxation decays of the ENMR signals.

EXPERIMENTAL

The 2D CT-STE-ENMR experiments were carried out at 25°C on a Bruker AM 500-MHz NMR spectrometer equipped with an actively shielded magnetic field gradient in the z -axis. A CA-ENMR sample cell was assembled using 12 U-shaped capillaries (I.D. = $250 \mu\text{m}$) (22). The inner glass surface of the sample cell was treated with HCl (1 M), distilled water, and NaOH (1 M) before use. Two platinum electrodes were inserted into the solution reservoirs in the two Teflon containers at the end of the

capillary arms. The sample assembly was lowered from the top of the magnet into a commercial 5-mm gradient probe. The DC electric field was generated in constant-current mode from an electric-gradient generator (Digital Specialties, Inc.), with a rising time of 1 ms/mA at a maximum output voltage of 1 kV . The pulsed magnetic field gradients were produced from the same device with a rising time of $10 \mu\text{s}$. The triggers controlled by the Bruker CT-STE-ENMR pulse sequence program determined the onsets of the electric field and gradient pulses. The amplitude and duration of an electric field pulse, as well as the amplitude of the gradient pulses, were defined in the electric field-gradient driver program installed in an IBM PC 486 computer. Since only electric field pulses of constant amplitudes are required, the CT-ENMR method is less hardware demanding than the previous EF-amplitude-incrementing 2D ENMR methods.

RESULTS

To demonstrate the effectiveness and capability of the CT-ENMR method, a sample solution was prepared to contain a mixture of 100 mM 4,9-dioxa-1,12-dodecanediamine and 100 mM L-aspartic acid in D_2O . The solution conductivity (κ) was $5.3 \text{ mS} \cdot \text{cm}^{-1}$. The 2D CT-STE-ENMR procedure was carried out with the following gradient and electric field parameters: $K = 570.2 \text{ cm}^{-1}$ and $E_{dc} = 57.7 \text{ V} \cdot \text{cm}^{-1}$, respectively. The duration of the DC electric field pulse (t_E) was stepwise increased from 8.51 to 1008.51 ms while the time delay, t_V , was stepwise decreased from 500 ms to $5 \mu\text{s}$ in 26 steps, in synchrony with the t_E incrementation (Fig. 1). The constant diffusion and relaxation time delays were set as $T_{Diff} = 1012.58 \text{ ms}$ and $T = 1008.51 \text{ ms}$, respectively, generating electrophoretic interferograms of constant amplitudes without diffusion and relaxation decays (Fig. 2a). Contributed from the electrophoretic migrations of ions and the bulk electroosmotic flow of the solution, the ionic migration rates of 4,9-dioxa-1,12-dodecanediamine and L-aspartic acids can be calculated as 1.15×10^{-4} and $1.71 \times 10^{-4} \text{ cm}^2 \cdot \text{V}^{-1} \cdot \text{s}^{-1}$, respectively, from the electrophoretic oscillation frequencies. In the Fourier domain, resonances from the two molecules can be displayed at resolved frequencies according to their electrophoretic mobilities ($I, 2$). Residual signal decays were observed in the flow dimension, which may originate from the heat-induced convection or other experimental imperfections (22, 24).

For comparison, a control experiment with the previous EF-time-incrementing 2D STE-ENMR sequence (Fig. 1) was carried out in similar experimental conditions. As the duration of the electric field pulse t_E was increased from 8.51 to 1008.51 ms , the diffusion time, t_{Diff} , changed from 12.68 to 1012.68 ms , and relaxation time, t_1 , changed from 8.61 to 1008.61 ms . Severe signal decays due to diffusion and relaxation were observed in the flow dimension (Fig. 2b). In the Fourier domain, the diffusion and relaxation line broadening would occur that degrades spectral resolution in the flow dimension.

TABLE 1
Simulated Electric Power Deposition and Electrophoretic Phase Changes in the CT-ENMR Method^a

t_E	8.5	108.5	208.5	308.5	408.5	508.5	608.5	708.5	808.5	908.5	1008.5
$I_e t_E$	8.5	108.5	208.5	308.5	408.5	508.5	608.5	708.5	808.5	908.5	1008.5
$I_e^2 t_E$	8.5	108.5	208.5	308.5	408.5	508.5	608.5	708.5	808.5	908.5	1008.5

^a The electric current $I_e = 1$ mA, and the unit of electric field duration t_E is ms.

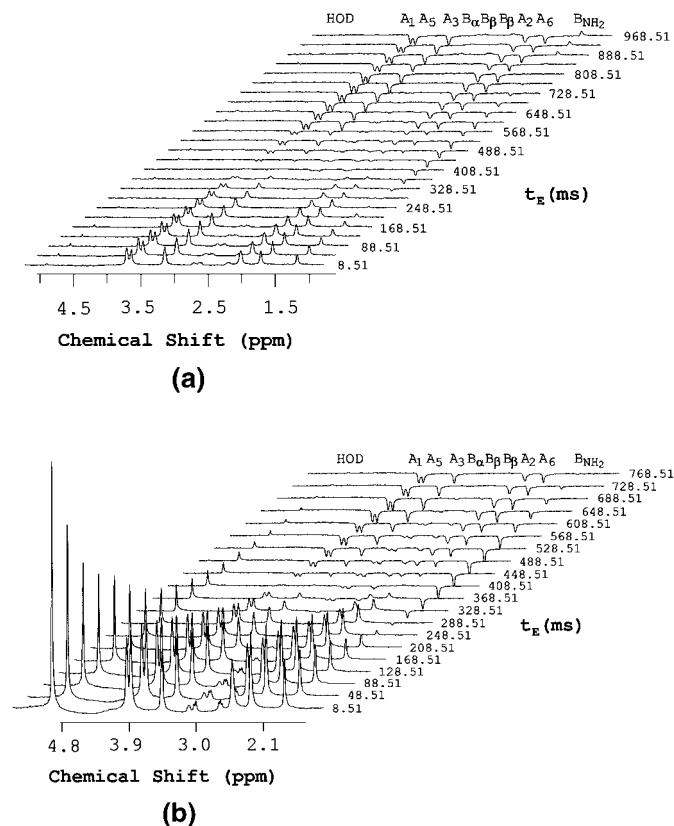


FIG. 2. (a) A stack plot of 2D CT-STE-ENMR spectra as a function of incrementing durations of the electric field pulse (t_E). Data were acquired at 25°C from a sample solution containing 100 mM L-aspartic acid and 100 mM 4,9-dioxo-1,12-dodecanediamine in D₂O. The solution conductivity (κ) was 5.3 mS · cm⁻¹. A U-shaped 12-bundle CA-ENMR (22) sample chamber was used with the capillary diameter of 250 μm. A constant electric field with amplitude of 57.7 V · cm⁻¹ was applied, corresponding to a constant electric current $I_e = 1.8$ mA. The electric field duration (t_E) was stepwise increased from 8.51 to 1008.51 ms, while the flanking t_v was stepwise decreased from 500 ms to 5 μs in 26 steps. The molecular diffusion time, $T_{Diff} = 1012.58$ ms, and the spin-lattice relaxation time period, $T = 1008.51$ ms, were set constant throughout the experiment. The encoding and decoding gradient amplitude and duration are $g = 21.32$ Gauss · cm⁻¹ and $\delta = 1$ ms, respectively. The spoil gradient has an amplitude $g_{sp} = 18.27$ Gauss · cm⁻¹ and duration $\delta_{sp} = 5$ ms. NS = 16, $\tau = 4.05$ ms, and $T_R = 3$ s. (b) The control STE-ENMR spectrum acquired from the same sample solution with NS = 8 for each spectrum. As the electric field pulse duration (t_E) was increased from 8.510 to 1008.51 ms, the molecular diffusion time (t_{Diff}) also increased from 12.68 to 1012.68 ms, while the spin-lattice relaxation time (t_1) increased from 8.61 to 1008.61 ms in 26 steps. A severe exponential signal decay was introduced due to molecular diffusion and spin relaxation effects. Other parameters were the same as in (a).

DISCUSSIONS

No obvious difference in heating and convection were observed in the CT-ENMR experiments from that in the EF-amplitude-incrementing ENMR. Since electric power deposition is $I_e^2 R t_E$ for a solution of resistance R , we have compared the calculated values of $I_e^2 t_E$ for electric power deposition or heating in a typical CT-ENMR experiment (Table 1) with that in an EF-amplitude-incrementing ENMR experiment (Table 2). The maximum electrophoretic flow induced phase change, represented by $I_e t_E$, was the same in both simulated experiments. A slightly more electric power deposition was predicted in CT-ENMR than in the EF-amplitude-incrementing ENMR method (Fig. 3). The maximum difference in electric power deposition in the two methods is 0.1314 J for a capillary array U-tube of length $L = 16$ cm and solution resistance $R = L/\kappa A = 512.5$ kΩ. This difference in heating is negligibly small, which is consistent with our experimental observations considering that the heat exchange of the CA-ENMR sample assembly is extremely efficient with cooling air flowing between the capillaries. The CA-ENMR setup dramatically reduces solution convection because of the physical barriers imposed by the capillary walls (22).

CT-ENMR is particularly advantageous when the DC electric field is applied to the xy -magnetization (as in a spin-echo ENMR experiment), not parallel to the static magnetic field B_0 . Such a configuration was used in the pioneering ENMR experiments carried out on an electromagnetic NMR spectrometer where the DC electric field was perpendicular to the B_0 direction (12–14). The electric current (I_e) not parallel to B_0 produces

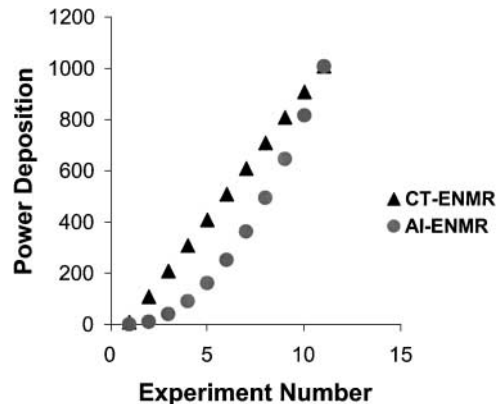


FIG. 3. Calculated electric power deposition or heating in (a) the CT-ENMR and (b) the EF-amplitude-incrementing ENMR (AI-ENMR). The maximum spectral phase change was the same in both experiments.

TABLE 2

Simulated Electric Power Deposition and Electrophoretic Phase Changes in the EF-Amplitude-Incrementing ENMR Method^a

I_e	0	0.1	0.2	0.3	0.4	0.5	0.6	0.7	0.8	0.9	1.0
$I_e t_E$	0	100.85	201.7	302.55	403.40	504.25	605.10	705.95	806.80	907.65	1008.5
$I_e^2 t_E$	0	10.085	40.34	90.76	161.36	252.13	363.06	494.17	645.44	816.89	1008.5

^a The electric field duration $t_E = 1008.5$ ms, and the unit of the electric current I_e is mA.

an additional magnetic field gradient, causing undesirable phase changes of the xy -magnetization that are superimposed to the electrophoretic phase modulations to be measured in the flow dimension. Since the induced gradient strength changes when the amplitude of electric field is incrementing, special hardware compensations or careful signal processing algorithms are required for reliable ENMR measurements in such EF-amplitude-incrementing ENMR experiments. In the CT-ENMR experiments, however, signal phase distortions from the DC electric field induced gradient would not cause severe problems. Because constant electric current is applied to the xy -magnetization, the electric current induced spectral phase modulations are the same throughout a CT-ENMR experiment and, therefore, can be corrected using routine NMR signal processing procedures. In the special case of the 2D STE-ENMR experiment, the electric field pulse is applied between the second and the third 90° pulses when the magnetization is stored in the z -direction. The electric current induced magnetic field gradient does not alter the pattern of electrophoretic phase modulation but simply dephases the remaining magnetization in the xy -plane (as a spoil gradient). Therefore, the electric field can be applied in any orientations relative to the B_0 field. In our ENMR experiments on a vertical superconducting NMR spectrometer, the electric field is applied parallel to the static magnetic field, B_0 , which does not induce magnetic field gradient. In general, the CT-ENMR strategy permits novel experiments in which the electric field can be applied in arbitrary orientations relative to the B_0 direc-

tion. For example, ENMR probes using cylindrical sample cells can be designed (Fig. 4) to be free from the electrolysis induced bubble disturbance at the receiver coil region, permitting effective separation of signals from ionic species moving in opposite directions.

CONCLUSIONS

Constant-time multidimensional electrophoretic NMR has been developed to enhance spectral resolution in the flow dimension using an EF-time-incrementing ENMR method. The undesirable diffusion and relaxation signal decays have been reduced to a constant amplitude factor by keeping constant the time delays between the encoding and decoding gradients and between the RF pulses. Since only an electric field of constant amplitude is required in CT-ENMR, the method produces constant phase shifts of NMR resonances when the electric field is applied not parallel to the static magnetic field B_0 to the xy -magnetization. In general, such capability permits new designs of ENMR probes and sample chambers to effectively remove bubbles induced by electrolysis at the two electrodes. The CT-ENMR is particularly useful in cases when the EF-amplitude-incrementing method is not applicable. The technical achievements of CT-ENMR have enhanced our strength to advance the multidimensional ENMR methods for structural characterization of multiple protein conformations and protein interactions.

ACKNOWLEDGEMENTS

The work was supported in part by grants from the National Science Foundation (NSF MCB-9707550), the National Institutes of Health (NIH RR12774-01), the American Chemical Society Petroleum Research Funds (PRF 32308-G4), and the University of Connecticut Research Foundation (Grant 441833). We thank Drs. Manfred Holz at the University of Karlsruhe in Germany for discussions, Douglas L. Rothman at the Magnetic Resonance Center, Yale University School of Medicine for making available the Bruker 500 MHz NMR spectrometer, and T. C. Ting at the University of Connecticut for reading the manuscript. The task was initiated and partially conducted in the Department of Chemistry, University of Connecticut.

REFERENCES

1. Q. He and C. S. Johnson, Jr., Two-dimensional electrophoretic NMR for the measurement of mobilities and diffusion in mixtures, *J. Magn. Reson.* **81**, 435 (1989).
2. Q. He and C. S. Johnson, Jr., Stimulated echo electrophoretic NMR, *J. Magn. Reson.* **85**, 181–185 (1989).

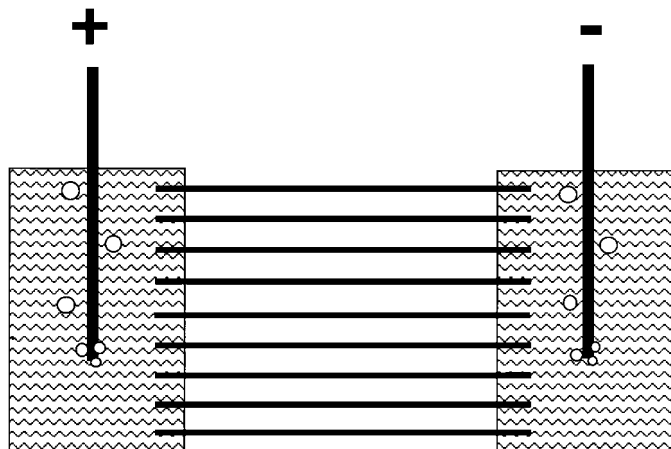


FIG. 4. A novel horizontal CA-ENMR sample cell design which prevents signal interference from bubbles generated at the two electrodes. The signal can be detected in a solenoidal coil wound around the capillary bundle.

3. Q. He, D. P. Hinton, and C. S. Johnson, Jr., Measurement of mobility distributions for vesicles by electrophoretic NMR, *J. Magn. Reson.* **91**, 654–658 (1991).
4. F. M. Coveney, J. H. Strange, A. L. Smith, and E. G. Smith, NMR studies of electrophoretic mobility in surfactant systems, *Colloids Surf.* **36**, 193–198 (1989).
5. C. S. Johnson, Jr., and Q. He, Electrophoretic NMR, in “Advanced Magnetic Resonance” (W. S. Warren, Eds), p. 131–159, Academic Press, San Diego (1989).
6. Q. He, “Electrophoretic Nuclear Magnetic Resonance,” Ph.D. thesis, University of North Carolina at Chapel Hill, 1990.
7. S. R. Heil and M. Holz, Electrical transport in a disordered medium: NMR measurement of diffusivity and electrical mobility of ionic charge carriers, *J. Magn. Reson.* **135**, 17–22 (1998).
8. T. R. Saarinen and C. S. Johnson, Jr., High-resolution electrophoretic NMR, *J. Am. Chem. Soc.* **110**, 3332 (1988).
9. M. Holz, D. Seiferling, and X. Mao, Design of a new electrophoretic NMR probe and its application to ${}^7\text{Li}^+$ and ${}^{133}\text{Cs}^+$ mobility studies, *J. Magn. Reson. Ser. A* **105**, 90–94 (1993).
10. M. Holz, Electrophoretic NMR, *Chem. Soc. Rev.* **23**, 165–174 (1994).
11. S. R. Heil and M. Holz, A mobility filter for the detection and identification of charged species in complex liquid mixtures by ENMR phase difference spectroscopy, *Angew. Chem. Int. Ed. Engl.* **35**, 1717–1720 (1996).
12. M. Holz and C. Muller, NMR measurement of internal magnetic field gradients caused by the presence of an electric current in electrolyte solutions, *J. Magn. Reson.* **40**, 595–599 (1980).
13. M. Holz and C. Muller, Direct measurement of single ionic drift velocities in electrolyte solutions: An NMR method, *Ber. Bunsenges. Phys. Chem.* **86**, 141–147 (1982).
14. M. Holz, O. Lucas, and C. Muller, NMR in the presence of an electric current: Simultaneous measurements of ionic mobilities, transfer numbers, and self-diffusion coefficients using an NMR pulsed-gradient experiment, *J. Magn. Reson.* **58**, 294–305 (1984).
15. M. Holz, C. Muller, and A. M. Wachter, Modification of the pulsed magnetic field gradient method for the determination of low velocities by NMR, *J. Magn. Reson.* **69**, 108–115 (1986).
16. C. S. Johnson, Jr., Electrophoretic NMR, in “Encyclopedia of NMR” (D. Grant, Ed.), pp. 1886–1895, Wiley, New York (1995).
17. K. F. Morris and C. S. Johnson, Jr., Mobility-ordered 2D NMR spectroscopy for the analysis of ionic mixtures, *J. Magn. Reson., Ser. A* **100**, 67–73 (1993).
18. K. F. Morris and C. S. Johnson, Jr., Mobility-ordered two-dimensional nuclear magnetic resonance spectroscopy, *J. Am. Chem. Soc.* **114**, 776–777 (1992).
19. J. H. Strange, E. G. Smith, and F. M. Coveney, “NMR Apparatus and Method for Electrophoretic Mobility,” European Patent 0 361 942 A2 (1989).
20. H. Dai and T. A. Zawodzinski, Jr., Determination of lithium ion transference numbers by electrophoretic nuclear magnetic resonance, *J. Electrochem. Soc.* **143**, L107–L109 (1996).
21. Q. He, Y. Liu, and T. Nixon, High-Field Electrophoretic NMR of Mixed Proteins in Solution, *J. Am. Chem. Soc.* **120**, 1341–1342 (1998).
22. Q. He, Y. Liu, H. Sun, and E. Li, Capillary array electrophoretic NMR of proteins in biological buffer solutions, *J. Magn. Reson.* **141**, 355–359 (1999).
23. Q. He, W. Lin, Y. Liu, and E. Li, Three-dimensional electrophoretic NMR correlation spectroscopy, *J. Magn. Reson.* **147**, 361–365 (2000).
24. Q. He and Z. Wei, Convection compensated electrophoretic NMR, *J. Magn. Reson.* **150**, 126–131 (2001).